



Refined model of stiffened shells

V.V. Karpov, A.A. Semenov*

Saint Petersburg State University of Architecture and Civil Engineering, Information Technologies, 4, 2nd Krasnoarmeyskaya st., 190005 Saint-Petersburg Russian Federation

ARTICLE INFO

Article history:

Received 1 November 2019

Revised 20 March 2020

Accepted 23 March 2020

Available online 12 May 2020

Keywords:

Shells

Buckling

Mathematical model

Stiffened ribs

ABSTRACT

The paper addresses several existing versions of mathematical models describing stiffened shell structures (accounting for the interaction between stiffeners and skin “along a line”, and “along a strip”, and a method for “smearing” the stiffness of stiffeners over the entire structure). The authors suggest a new, most accurate version to account for stiffness properties of stiffeners, based on introducing various modular ratios along various coordinate axes. For stiffeners perpendicular to the direction under consideration, the authors introduce a modular ratio equal to the ratio between the width of stiffeners in this direction and the linear dimension of the shell in the direction under consideration. For analysis, the authors use an algorithm based on the Ritz method and the best parameter continuation method. Three versions of models, taking into account the discrete introduction of stiffeners, are compared. Analysis is performed for isotropic shallow doubly curved shells reinforced with an orthogonal grid of stiffeners.

© 2020 Elsevier Ltd. All rights reserved.

1. Introduction

Shell structures are widely applied in various industries, including civil engineering and machine engineering. Thin-walled shells have a particular weakness: they actually can lose stability. To avoid this, they are reinforced with stiffeners (Cho et al., 2019, Bushnell and Bushnell, 1996, Solovei et al., 2015, Lutskeya et al., 2016, Xu et al., 2016), which can significantly increase their critical load, redistribute critical stresses and, therefore, improve structural performance.

The foundations for the design of stiffened shells were formulated in the late 1940s by (Lurie, 1948) and Vlasov (Vlasov, 1949). Both Lurie and Vlasov believed that stiffeners interact with the skin along a line and represent one-dimensional rod elements that can resist only tension/compression and bending. Vlasov considered the interaction of the stiffeners and the skin to be a contact problem. Lurie considered the shell and the stiffeners as a single system and obtained stiffened shell equilibrium equations based on the condition for the minimum total deformation energy functional. The third approach to the stiffened shell is based on “smearing” the stiffness of the stiffeners over the entire shell and considering it to be structurally orthotropic.

In his paper, (Van der Neut, 1947) pointed out the importance of stiffeners' eccentricity when stability is lost under axial compression. It was one of the first papers addressing the stability of

eccentrically stiffened closed cylindrical shells. He also made an important conclusion: in such structures, the buckling load of an externally stiffened shell can be as high as two or three times that of an internally stiffened shell.

Among the papers of that period, papers by (Baruch and Singer, 1963); Block, Card, and Mikulas (Block et al., August 1965), and Singer et al. (Singer et al., 1967) are notable.

Kidane et al. (Kidane et al., 2003) determined the global buckling load for various versions of grid stiffened cylindrical shells with fixed pin joints along the contour and anchorage.

McElman, Mikulas, and Stein (McElman et al., 1966) considered the effect of stiffening on vibrations and flutter. Vibrations were also considered by (Lee and Kim, 1998, Lee and Kim, 1999), (Zhao et al., 2002), and Talebitooti et al. (Talebitooti et al., 2010). Prusty (Prusty, 2008) analyzed free vibration and buckling response of stiffened panels under general loading. Dynamic problems were also considered in papers (Abramovich and Zarutskii, 2008, Meish and Kairov, 2005, Shulga and S.Yu, 2003, Suleymanova, 2007, Belikov and S.Yu, 2011, Dyachenko et al., 2011, Latifov and Suleymanova, 2009, Mehtiyev, 2011, Nazarov, 1965, Nemchinov Yu. and Talbatov Yu, 1975, Seyfullayev and Novruzova, 2015, Abramovich and Zarutskii, 2010).

Optimization of stiffened cylindrical shells to solve specific practical tasks was addressed by Bai et al. (Bai et al., 2017), Jarmai et al. (Jarmai et al., 2006), Simoes et al. (Simoes et al., 2006), Chen et al. (Chen et al., 2008), Lene et al. (Lene et al., 2009), Smerdov (Smerdov, 2014), and Hao et al. (Hao et al., 2017).

It is significantly more difficult to study stiffened structures than structures of uniform thickness. In this regard, there are sev-

* Corresponding Author

E-mail address: sw.semenov@gmail.com (A.A. Semenov).

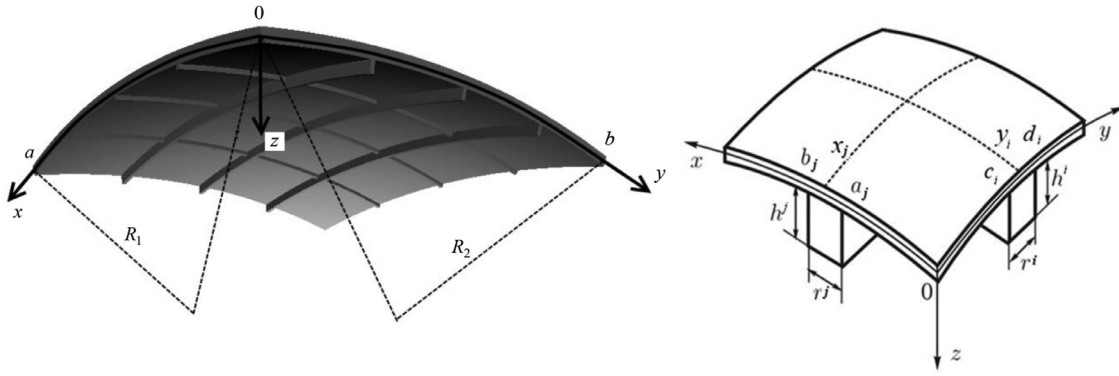


Fig. 1. Layout view of a stiffened doubly curved shell.

eral approaches to the introduction of stiffeners. For instance, some papers (Kidane et al., 2003, Jaunky et al., 1996) distinguish three types of approaches to account for stiffeners in a structure: a discrete approach (Wang and Hsu, 1985) (Wang and Hsu, 1985), the branched plate and shell approach, and a stiffness smearing approach [40–43 and others] (Dow, Libove, and Hubka, 1953; Troitsky, 1976; Reddy, Valisetty, and Rehfield, 1985; Jaunky, 1992).

Reviews of literature on stiffened shells can be found in some prominent papers (Jaunky et al., 1996, Wang et al., 2016, Buragohain and Velmurugan, 2009, Jones, 1968, Sadeghifar et al., 2011, Ren et al., 2014).

The purpose of this paper is to analyze the existing models of stiffened shells and to develop a new, more accurate model.

2. Theory

2.1. Geometry of the structures under consideration

Shells of arbitrary form under equally distributed external transverse load $q = q(x, y)$, are examined. The middle surface of a shell having thickness h is considered the coordinate surface. The x and y axes are oriented along the main shell curvature lines, and the z axis is oriented along the normal to the middle surface in the direction of the concavity (e.g. a shallow doubly curved shell is shown in Fig. 1).

2.2. Mathematical model of skin deformation

Let us consider the shell deformation model of the Timoshenko (Mindlin–Reissner) type. Then, displacements in the layer at a distance z from the middle surface will be as follows:

$$U^z = U + z\Psi_x, \quad V^z = V + z\Psi_y, \quad W^z = W. \quad (1)$$

Here, $U = U(x, y)$, $V = V(x, y)$, $W = W(x, y)$ are unknown displacement functions, and $\Psi_x = \Psi_x(x, y)$, $\Psi_y = \Psi_y(x, y)$ are unknown functions of the normal rotation angles in the xOz and yOz planes, respectively.

The mathematical model of shell structure deformation can be based on equilibrium equations or the functional of full potential deformation energy. Let us consider the model based on the functional, as its order of derivatives is half that in equilibrium equations, which simplifies calculation.

When calculating geometrical nonlinearity and transverse shears, geometrical relationships (between deformation and displacement components) in the middle surface of the shell will take

the following form:

$$\begin{aligned} \varepsilon_x &= \frac{1}{A} \frac{\partial U}{\partial x} + \frac{1}{AB} V \frac{\partial A}{\partial y} - k_x W + \frac{1}{2} \theta_1^2, \\ \varepsilon_y &= \frac{1}{B} \frac{\partial V}{\partial y} + \frac{1}{AB} U \frac{\partial B}{\partial x} - k_y W + \frac{1}{2} \theta_2^2, \\ \gamma_{xy} &= \frac{1}{A} \frac{\partial V}{\partial x} + \frac{1}{B} \frac{\partial U}{\partial y} - \frac{1}{AB} U \frac{\partial A}{\partial y} - \frac{1}{AB} V \frac{\partial B}{\partial x} + \theta_1 \theta_2, \\ \gamma_{xz} &= k f(z) [\Psi_x - \theta_1], \quad \gamma_{yz} = k f(z) [\Psi_y - \theta_2], \\ \theta_1 &= -\left(\frac{1}{A} \frac{\partial W}{\partial x} + k_x U \right), \quad \theta_2 = -\left(\frac{1}{B} \frac{\partial W}{\partial y} + k_y V \right), \end{aligned} \quad (2)$$

and curvature and torsion functions will be as follows:

$$\begin{aligned} \chi_1 &= \frac{1}{A} \frac{\partial \Psi_x}{\partial x}, \quad \chi_2 = \frac{1}{B} \frac{\partial \Psi_y}{\partial y} + \frac{1}{AB} \frac{\partial B}{\partial x} \Psi_x, \\ \chi_{12} &= \frac{1}{2} \left(\frac{1}{A} \frac{\partial \Psi_y}{\partial x} + \frac{1}{B} \frac{\partial \Psi_x}{\partial y} - \frac{1}{AB} \frac{\partial B}{\partial x} \Psi_y \right), \end{aligned} \quad (3)$$

where $\varepsilon_x, \varepsilon_y$ are the strain deformations along the x, y coordinates of the middle surface; $\gamma_{xy}, \gamma_{xz}, \gamma_{yz}$ are the shear deformations in the xOy, xOz, yOz planes, respectively; k_x, k_y are the main curvatures of the shell along the x and y axes that characterize its geometry; A, B are the Lamé parameters; $f(z)$ is the function describing the distribution of stresses τ_{xz} and τ_{yz} through the skin thickness; and $k = 5/6$.

For the layer of skin located at a distance z from the middle surface, deformations will be as follows:

$$\varepsilon_x^z = \varepsilon_x + z\chi_1, \quad \varepsilon_y^z = \varepsilon_y + z\chi_2, \quad \gamma_{xy}^z = \gamma_{xy} + 2z\chi_{12}. \quad (4)$$

Physical relationships (between stresses and deformations) for an orthotropic material in the event of linear–elastic deformations are written as follows (Semenov, 2016):

$$\begin{aligned} \sigma_x &= \frac{E_1}{1-\mu_{12}\mu_{21}} [\varepsilon_x + \mu_{21}\varepsilon_y + z(\chi_1 + \mu_{21}\chi_2)], \\ \sigma_y &= \frac{E_2}{1-\mu_{12}\mu_{21}} [\varepsilon_y + \mu_{12}\varepsilon_x + z(\chi_2 + \mu_{12}\chi_1)], \\ \tau_{xy} &= G_{12}[\gamma_{xy} + 2z\chi_{12}], \quad \tau_{xz} = G_{13}\gamma_{xz}; \quad \tau_{yz} = G_{23}\gamma_{yz}. \end{aligned} \quad (5)$$

The direction of the orthotropy axis 1 coincides with the direction of the x axis, and for other directions, the coordinate system needs to be rotated.

Here, $E_1, E_2, \mu_{12}, \mu_{21}, G_{12}, G_{13}, G_{23}$ are mechanical properties of the material. In case of an isotropic material, assume $E_1 = E_2 = E$, $\mu_{12} = \mu_{21} = \mu$, $G_{12} = G_{13} = G_{23} = G$.

Equations for forces and moments can be found by integrating stresses with respect to z from $-h/2$ to $h/2$ (for force factors acting in the skin).

In the skin, the cross-section area per unit of cross-section length will be the same in the direction of the x and y axes, and equal to $\int_{-h/2}^{h/2} dz = h$; the static moment of the cross-section per unit of cross-section length will be equal to $\int_{-h/2}^{h/2} z dz = 0$; the moment of cross-section inertia per unit of cross-section length will be equal to $\int_{-h/2}^{h/2} z^2 dz = \frac{h^3}{12}$.

Therefore, the components of forces and moments acting in the skin (superscript "0") will take the following form:

$$\begin{aligned} N_x^0 &= G_1^0 h(\varepsilon_x + \mu_{21} \varepsilon_y), \quad N_y^0 = G_2^0 h(\varepsilon_y + \mu_{12} \varepsilon_x), \\ M_x^0 &= G_1^0 \frac{h^3}{12} (\chi_1 + \mu_{21} \chi_2), \\ M_y^0 &= G_2^0 \frac{h^3}{12} (\chi_2 + \mu_{12} \chi_1), \quad N_{xy}^0 = G_{12}^0 h \gamma_{xy}, \\ M_{xy}^0 &= G_{12}^0 2 \frac{h^3}{12} \chi_{12}, \quad Q_x^0 = k G_{13}^0 h(\Psi_x - \theta_1), \quad Q_y^0 = k G_{23}^0 h(\Psi_y - \theta_2), \end{aligned} \quad (6)$$

where:

$$G_1^0 = \frac{E_1}{1 - \mu_{12} \mu_{21}}, \quad G_2^0 = \frac{E_2}{1 - \mu_{12} \mu_{21}},$$

The functional of full potential deformation energy of the shell structure can be written in the following form:

$$E_s = E_s^0 + E_s^R, \quad (7)$$

where E_s^R depends on the method for defining the stiffeners, taking the following form:

$$\begin{aligned} E_s^R &= \frac{1}{2} \int_{a_1}^a \int_0^b \left[N_x^R \varepsilon_x + N_y^R \varepsilon_y + \frac{1}{2} (N_{xy}^R + N_{yx}^R) \gamma_{xy} + M_x^R \chi_1 + M_y^R \chi_2 + (M_{xy}^R + M_{yx}^R) \chi_{12} \right. \\ &\quad \left. + Q_x^R (\Psi_x - \theta_1) + Q_y^R (\Psi_y - \theta_2) \right] AB dx dy, \end{aligned} \quad (8)$$

and the part of the functional associated with the skin will be as follows:

$$\begin{aligned} E_s^0 &= \frac{1}{2} \int_{a_1}^a \int_0^b \left[N_x^0 \varepsilon_x + N_y^0 \varepsilon_y + N_{xy}^0 \gamma_{xy} + M_x^0 \chi_1 + M_y^0 \chi_2 + 2 M_{xy}^0 \chi_{12} + Q_x^0 (\Psi_x - \theta_1) \right. \\ &\quad \left. + Q_y^0 (\Psi_y - \theta_2) - 2 q W \right] AB dx dy. \end{aligned} \quad (9)$$

2.3. Model of a stiffened shell in contact with the skin along a line

The approaches suggested by Lurie and Vlasov are used in numerous papers addressing stiffened shells (Amiro and Zarutsky, Greben, Mikhaylov, Mileyskovsky and Grechaninov, Terebushko, Timashev et al.). Among the authors listed above, only Terebushko used Vlasov's approach. The others used Lurie's approach, presenting forces and moments acting in stiffeners as follows:

$$\begin{aligned} N_x^R &= E_1 \sum_{i=1}^n (F^i r_i \varepsilon_x + S^i r_i \chi_1) \delta(y - y_i), \\ N_y^R &= E_2 \sum_{j=1}^m (F^j r_j \varepsilon_y + S^j r_j \chi_2) \delta(x - x_j), \quad N_{xy}^R = 0, \\ M_x^R &= E_1 \sum_{i=1}^n (S^i r_i \varepsilon_x + J^i r_i \chi_1) \delta(y - y_i), \\ M_y^R &= E_2 \sum_{j=1}^m (S^j r_j \varepsilon_y + J^j r_j \chi_2) \delta(x - x_j), \quad M_{xy}^R = 0, \\ Q_x^R &= 0, \quad Q_y^R = 0. \end{aligned} \quad (10)$$

Here, F^i, S^i, J^i, r_i, n are the cross-section area of stiffeners per unit of cross-section length, for stiffeners parallel to the x axis; the static moment and the moment of inertia of that cross-section; the width of stiffeners in this direction and the number of stiffeners in this direction. Similarly, F^j, S^j, J^j, r_j, m are for stiffeners parallel to the y axis, and $\delta(x - x_j), \delta(y - y_i)$ are delta functions.

Introducing stiffeners along a line simplifies the mathematical model of the shell, but ultimately neglects many important physical factors, affecting the accuracy of the resulting solutions. For instance, the impact of stiffeners on shear and torsion in the middle surface of the shell is neglected; where they intersect, stiffeners do not affect each other at all.

2.4. Model of a stiffened shell in contact with the skin along a strip

In the late 1960s, Zhilin suggested considering a stiffened shell as a shell of discrete and variable thickness. A similar approach was used in papers by Endzhievsky, Preobrazhensky, and Karpov.

In a paper by Endzhievsky (Endzhievsky, 1982), Eq. (10) are taken for narrow stiffeners, and the surfaces $z_1(x, y) = -h/2$ and $z_2(x, y) = h/2 + \sum_{i=1}^n h^i \Gamma_0^*(y_i) + \sum_{j=1}^m h^j \Gamma_0^*(x_j)$ are considered for wide stiffeners, where h^i, h^j are the height of the stiffeners in two directions, and $\Gamma_0^*(y_i), \Gamma_0^*(x_j)$ are, in effect, the differences between two unit functions at the corresponding width of the stiffener. The equations also take into account that the common portion of intersecting stiffeners is subtracted.

The forces and moments acting in the skin and stiffeners are calculated in paper (Endzhievsky, 1982) as follows (for an isotropic material, i.e. $E_1 = E_2 = E$, $\mu_{12} = \mu_{21} = \mu$):

$$\begin{aligned} N_x &= B^* \varepsilon_x + \mu B^* \varepsilon_y + C^* \chi_1 + \mu C^* \chi_2, \\ N_y &= B^* \varepsilon_y + \mu B^* \varepsilon_x + C^* \chi_2 + \mu C^* \chi_1, \\ N_{xy} &= \frac{1-\mu}{2} B^* \gamma_{xy} + (1-\mu) C^* \chi_{12}, \\ M_x &= C^* \varepsilon_x + \mu C^* \varepsilon_y + D^* \chi_1 + \mu D^* \chi_2, \\ M_y &= C^* \varepsilon_y + \mu C^* \varepsilon_x + D^* \chi_2 + \mu D^* \chi_1, \\ M_{xy} &= (1-\mu) C^* \gamma_{xy} + 2(1-\mu) D^* \chi_{12}. \end{aligned} \quad (11)$$

Here:

$$\begin{aligned} B^* &= \frac{E}{1-\mu^2} \left(h + \sum_{i=1}^n h^i \Gamma_0^*(y_i) + \sum_{j=1}^m h^j \Gamma_0^*(x_j) \right), \\ C^* &= \frac{E}{1-\mu^2} \left(\sum_{i=1}^n h^i \eta_i \Gamma_0^*(y_i) + \sum_{j=1}^m h^j \eta_j \Gamma_0^*(x_j) \right), \\ D^* &= \frac{E}{12(1-\mu^2)} \left(h^3 + \sum_{i=1}^n \left((h^i)^3 + h^i \eta_i^2 \right) \Gamma_0^*(y_i) + \sum_{j=1}^m \left((h^j)^3 + h^j \eta_j^2 \right) \Gamma_0^*(x_j) \right), \end{aligned} \quad (12)$$

where η_i, η_j is the distance from the middle surface of the shell to the center of gravity of the stiffener.

Therefore, using the notations in this paper, the forces and moments acting only in the stiffeners will be as follows:

$$\begin{aligned} N_x^R &= G_1^R (F^* (\varepsilon_x + \mu \varepsilon_y) + S^* (\chi_1 + \mu \chi_2)), \\ N_y^R &= G_2^R (F^* (\varepsilon_y + \mu \varepsilon_x) + S^* (\chi_2 + \mu \chi_1)), \\ N_{xy}^R &= G_{12}^R (F^* \gamma_{xy} + 2S^* \chi_{12}), \\ M_x^R &= G_1^R (S^* (\varepsilon_x + \mu \varepsilon_y) + J^* (\chi_1 + \mu \chi_2)), \\ M_y^R &= G_2^R (S^* (\varepsilon_y + \mu \varepsilon_x) + J^* (\chi_2 + \mu \chi_1)), \\ M_{xy}^R &= G_{12}^R (2S^* \gamma_{xy} + 4J^* \chi_{12}). \end{aligned} \quad (13)$$

Here:

$$\begin{aligned} F^* &= \sum_{i=1}^n h^i \Gamma_0^*(y_i) + \sum_{j=1}^m h^j \Gamma_0^*(x_j), \\ S^* &= \sum_{i=1}^n h^i \eta_i \Gamma_0^*(y_i) + \sum_{j=1}^m h^j \eta_j \Gamma_0^*(x_j), \\ J^* &= \frac{1}{12} \left(\sum_{i=1}^n \left((h^i)^3 + h^i \eta_i^2 \right) \Gamma_0^*(y_i) + \sum_{j=1}^m \left((h^j)^3 + h^j \eta_j^2 \right) \Gamma_0^*(x_j) \right). \end{aligned} \quad (14)$$

Since the version of the model described in paper (Endzhievsky, 1982) is developed for an isotropic material, we must assume $G_1^R = G_2^R = \frac{E}{1-\mu^2}$, $G_{12}^R = G_{13}^R = G_{23}^R = \frac{E}{2(1+\mu)}$.

In effect, stiffness properties of stiffeners depend on the area of cross-section or longitudinal section per unit of section length, static moment, and moment of inertia of that section.

Karpov developed a geometrically nonlinear model for shells of stepped variable thickness that have stiffeners, reinforcement plates, and cutouts, taking into account the discrete location and width of stiffeners and cutouts, interaction between the stiffeners and skin along a strip, rigid intersection of stiffeners, shear and torsional rigidity of stiffeners, transverse shears, i.e. all the most important factors affecting the stress-strain state and buckling of shells that had previously been neglected due to the complexity of calculation. He proved that Vlasov's and Lurie's approaches to designing stiffened shells are equivalent.

The discrete layer of shell stiffeners is described by the function $H(x, y)$, which characterizes the height and location of the stiffeners with regard to the shell.

$$H(x, y) = \sum_{j=1}^m h^j \bar{\delta}(x - x_j) + \sum_{i=1}^n h^i \bar{\delta}(y - y_i) - \sum_{i=1}^n \sum_{j=1}^m h^{ij} \bar{\delta}(x - x_j) \bar{\delta}(y - y_i), \quad (15)$$

where h^i, h^j are the height of stiffeners; i and j indicate stiffeners parallel to the x and y axes, respectively; n, m are the number of stiffeners; $h^{ij} = \min\{h^i, h^j\}$, i.e. the common portion of intersecting stiffeners; $\bar{\delta}(x - x_j)$ and $\bar{\delta}(y - y_i)$ are unit column functions representing the differences between unit functions $\bar{\delta}(x - x_j) = U(x - a_j) - U(x - b_j)$; $\bar{\delta}(y - y_i) = U(y - c_i) - U(y - d_i)$, where $a_j = x_j - r_j/(2A)$, $b_j = x_j + r_j/(2A)$, $c_i = y_i - r_i/(2B)$, $d_i = y_i + r_i/(2B)$ (width of stiffeners r_i, r_j is given in meters for any rotational shells).

Since the Lamé parameter A is constant for rotational shells, and the Lamé parameter B equals $B(x)$, then a_j, b_j , are constants. To ensure the same width of the i^{th} stiffeners at any x , $c_i = c_i(x)$, $d_i = d_i(x)$.

If we define the location of the stiffeners in such manner, the contact between the skin and stiffeners will be along a strip. Where they intersect, stiffeners are rigidly fixed against each other. Therefore, the thickness of the entire structure equals $h + H$, where h is the thickness of the skin.

In his papers, Karpov (Ilyin and Karpov, 1986, Karpov, 2018) demonstrates that the limiting transition (in terms of the functional of full potential deformation energy of the shell) from unit column functions $\bar{\delta}(x - x_j), \bar{\delta}(y - y_i)$ to delta functions $\delta(x - x_j), \delta(y - y_i)$ yields the ratio obtained previously, when the contact of the skin and stiffeners is along a line.

It has been proven that the boundary conditions of the free edge are satisfied on the lateral surface of stiffeners. Therefore, if we assume $h^j = 0, h^i = 0, h^{ij} = h$, we will get a version of shells weakened by cutout holes. Since the free boundary condition is satisfied automatically at the edge of the cutout, then, for shells weakened by cutouts, we will get a set of equations for a simply connected region, which simplifies its solution significantly.

A computational experiment has demonstrated that if there are stiffeners in the shell, accounting for transverse shears affects the stress-strain state significantly.

It is natural to assume that, in case of force factors acting in stiffeners, stiffness properties can be determined by integrating with respect to z from $h/2$ to $h/2 + H$. Therefore:

$$\begin{aligned} \int_{h/2}^{h/2+H} dz &= \bar{F} = \sum_{i=1}^n F^i \bar{\delta}(y - y_i) + \sum_{j=1}^m F^j \bar{\delta}(x - x_j) - \sum_{i=1}^n \sum_{j=1}^m F^{ij} \bar{\delta}(x - x_j) \bar{\delta}(y - y_i), \\ \int_{h/2}^{h/2+H} z dz &= \bar{S} = \sum_{i=1}^n S^i \bar{\delta}(y - y_i) + \sum_{j=1}^m S^j \bar{\delta}(x - x_j) - \sum_{i=1}^n \sum_{j=1}^m S^{ij} \bar{\delta}(x - x_j) \bar{\delta}(y - y_i), \\ \int_{h/2}^{h/2+H} z^2 dz &= \bar{J} = \sum_{i=1}^n J^i \bar{\delta}(y - y_i) + \sum_{j=1}^m J^j \bar{\delta}(x - x_j) - \sum_{i=1}^n \sum_{j=1}^m J^{ij} \bar{\delta}(x - x_j) \bar{\delta}(y - y_i). \end{aligned} \quad (16)$$

Here:

$$\begin{aligned} F^i &= h^i, \quad F^j = h^j, \quad F^{ij} = h^{ij}, \\ S^i &= \frac{h^i(h+h^i)}{2}, \quad S^j = \frac{h^j(h+h^j)}{2}, \quad S^{ij} = \frac{h^{ij}(h+h^{ij})}{2}, \\ J^i &= 0.25h^2h^i + 0.5h(h^i)^2 + \frac{1}{3}(h^i)^3, \\ J^j &= 0.25h^2h^j + 0.5h(h^j)^2 + \frac{1}{3}(h^j)^3, \quad J^{ij} = 0.25h^2h^{ij} + 0.5h(h^{ij})^2 + \frac{1}{3}(h^{ij})^3. \end{aligned} \quad (17)$$

Therefore, the forces and moments acting in stiffeners will be as follows:

$$\begin{aligned} N_x^R &= G_1^R [\bar{F}(\varepsilon_x + \mu_{21}\varepsilon_y) + \bar{S}(\chi_1 + \mu_{21}\chi_2)], \\ N_y^R &= G_2^R [\bar{F}(\varepsilon_y + \mu_{12}\varepsilon_x) + \bar{S}(\chi_2 + \mu_{12}\chi_1)], \\ N_{xy}^R &= G_{12}^R [\bar{F}\gamma_{xy} + 2\bar{S}\chi_{12}], \quad N_{yx}^R = G_{12}^R [\bar{F}\gamma_{xy} + 2\bar{S}\chi_{12}], \\ M_x^R &= G_1^R [\bar{S}(\varepsilon_x + \mu_{21}\varepsilon_y) + \bar{J}(\chi_1 + \mu_{21}\chi_2)], \quad M_y^R = G_2^R [\bar{S}(\varepsilon_y + \mu_{12}\varepsilon_x) + \bar{J}(\chi_2 + \mu_{12}\chi_1)], \\ M_{xy}^R &= G_{12}^R [\bar{S}\gamma_{xy} + 2\bar{J}\chi_{12}], \quad M_{yx}^R = G_{12}^R [\bar{S}\gamma_{xy} + 2\bar{J}\chi_{12}], \\ Q_x^R &= G_{13}^R k\bar{F}(\Psi_x - \theta_1), \quad Q_y^R = G_{23}^R k\bar{F}(\Psi_y - \theta_2). \end{aligned} \quad (18)$$

2.5. Model of a stiffened shell with "smearing" of the stiffness of stiffeners

There are several ways to "smear" the stiffness of stiffeners over the entire shell. First, let us consider a version in which we neglect the impact of stiffeners on shear and torsion of the middle surface of the skin and do not take into account the mutual influence of stiffeners where they intersect. The following description in this section is taken from paper (Karmishin et al., 1975).

Stiffeners (eccentric) are characterized by the following values: F_i is the area of a stiffener; $S_i J_i$ are the static moment and moment of inertia of the stiffener cross-section relative to the axis crossing the middle surface of the skin, respectively; l_i is the average distance between stiffeners; E_1^0, E_2^0 is the stiffener modulus of elasticity (Karmishin et al., 1975).

$$\begin{aligned} N_{11} &= B_{11}(\varepsilon_1 + \mu\varepsilon_2) + A_{11}(\chi_1 + \mu\chi_2) \quad (1 \leftrightarrow 2), \\ N_{12} &= B_{33}\gamma_{12} + 2A_{33}\chi_{12}, \\ M_{11} &= A_{11}(\varepsilon_1 + \mu\varepsilon_2) + D_{11}(\chi_1 + \mu\chi_2) \quad (1 \leftrightarrow 2), \\ M_{12} &= A_{33}\gamma_{12} + 2D_{33}\chi_{12}. \end{aligned} \quad (19)$$

Let us write the equations for the stiffness coefficients as follows:

$$A_{ij} = \tilde{A}_{ij} + A_{ij}^0, \quad B_{ij} = \tilde{B}_{ij} + B_{ij}^0, \quad D_{ij} = \tilde{D}_{ij} + D_{ij}^0,$$

where $\tilde{A}_{ij}, \tilde{B}_{ij}, \tilde{D}_{ij}$ characterize the stiffness parameters of the skin, and $A_{ij}^0, B_{ij}^0, D_{ij}^0$ characterize the stiffness parameters of the stiffener reduced to the middle surface of the skin. The coefficients take the following form:

$$\begin{aligned} B_{ii}^0 &= \frac{E_i^0 F_i}{l_i} \quad (i = 1, 2), \quad B_{12}^0 = B_{21}^0 = B_{33}^0 = 0, \\ A_{ii}^0 &= \frac{E_i^0 S_i}{l_i} \quad (i = 1, 2), \quad A_{12}^0 = A_{21}^0 = A_{33}^0 = 0, \\ D_{ii}^0 &= \frac{E_i^0 J_i}{l_i} \quad (i = 1, 2), \quad D_{12}^0 = D_{21}^0 = D_{33}^0 = 0. \end{aligned} \quad (20)$$

If we define the distance from the center of gravity of the stiffener cross-section to the middle surface of the skin as z_{0i} , then:

$$S_i = F_i z_{0i}, \quad J_i = J_{0i} + z_{0i}^2 F_i, \quad (21)$$

where J_{0i} is the intrinsic moment of inertia of the stiffener cross-section.

Therefore, using the notations in this paper, the forces and moments acting only in the stiffeners will be as follows:

$$\begin{aligned} N_x^R &= \frac{E_1 F_1}{l_1} (\varepsilon_x + \mu \varepsilon_y) + \frac{E_1 S_1}{l_1} (\chi_1 + \mu \chi_2), \\ N_y^R &= \frac{E_2 F_2}{l_2} (\varepsilon_y + \mu \varepsilon_x) + \frac{E_2 S_2}{l_2} (\chi_2 + \mu \chi_1), \\ N_{xy}^R &= 0, \\ M_x^R &= \frac{E_1 S_1}{l_1} (\varepsilon_x + \mu \varepsilon_y) + \frac{E_1 J_1}{l_1} (\chi_1 + \mu \chi_2), \\ M_y^R &= \frac{E_2 S_2}{l_2} (\varepsilon_y + \mu \varepsilon_x) + \frac{E_2 J_2}{l_2} (\chi_2 + \mu \chi_1), \\ M_{xy}^R &= 0. \end{aligned} \quad (22)$$

This version of the model can be considered the first approximation to the solution of the problem under consideration.

2.6. Model of a stiffened shell with "smearing" of the stiffness of stiffeners using the method of structural anisotropy

Karpov developed a version of the method of structural anisotropy that takes into account shear and torsional stiffness of stiffeners.

Let us consider components of the force N_x^R for a shallow rectangular shell. The force in the direction of the x axis consists of $N_x^{LR} = \sum_{i=1}^n N_x^{Li} \delta(y - y_i)$ and $N_x^{BR} = \sum_{j=1}^m N_x^{Bj} \delta(x - x_j)$.

N_x^{LR} includes the stiffness of the i^{th} stiffeners parallel to the x axis and located at $0 \leq x \leq a$. Therefore, this component of N_x^R with reduced stiffness of stiffeners will be as follows (the modular ratio equals a/a)

$$N_x^{LR} \approx \sum_{i=1}^n \left(\frac{r_i}{b} N_x^{Li} \right) \frac{a}{a} = G_1^R \sum_{i=1}^n \left(\frac{F^i r_i}{b} (\varepsilon_x + \mu \varepsilon_y) + \frac{S^i r_i}{b} (\chi_1 + \mu \chi_2) \right). \quad (23)$$

N_x^{BR} includes the stiffness of the j^{th} stiffeners parallel to the y axis that, in the direction of the x axis, are located at $a_j \leq x \leq b_j$ ($b_j - a_j = r_j$), and "pieces" of stiffeners that represent the common portion of intersecting stiffeners oriented in different directions. Therefore, this component of N_x^R with reduced stiffness of stiffeners will be as follows (the modular ratio equals $\frac{r_j}{a}$)

$$\begin{aligned} N_x^{BR} &\approx \sum_{j=1}^m \left(\frac{r_j}{a} N_x^{Bj} \right) \frac{r_j}{a} = \\ &= G_1^R \sum_{j=1}^m \left[\left(\frac{F^j r_j}{a} - \sum_{i=1}^n \frac{F^{ij} r_i r_j}{ab} \right) \frac{r_j}{a} (\varepsilon_x + \mu \varepsilon_y) + \left(\frac{S^j r_j}{a} - \sum_{i=1}^n \frac{S^{ij} r_i r_j}{ab} \right) \frac{r_j}{a} (\chi_1 + \mu \chi_2) \right]. \end{aligned} \quad (24)$$

If we define

$$F_x = \sum_{i=1}^n \frac{F^i r_i}{b} + \sum_{j=1}^m \left(\frac{F^j r_j}{a} - \sum_{i=1}^n \frac{F^{ij} r_i r_j}{ab} \right) \frac{r_j}{a}, S_x = \sum_{i=1}^n \frac{S^i r_i}{b} + \sum_{j=1}^m \left(\frac{S^j r_j}{a} - \sum_{i=1}^n \frac{S^{ij} r_i r_j}{ab} \right) \frac{r_j}{a}, \quad (25)$$

then forces N_x^R (18) can be written as follows:

$$N_x^R = G_1^R (F_x (\varepsilon_x + \mu \varepsilon_y) + S_x (\chi_1 + \mu \chi_2)).$$

In a similar way, N_y^R can be written as follows:

$$N_y^R = G_2^R (F_y (\varepsilon_y + \mu \varepsilon_x) + S_y (\chi_2 + \mu \chi_1)),$$

where:

$$F_y = \sum_{j=1}^m \frac{F^j r_j}{a} + \sum_{i=1}^n \left(\frac{F^i r_i}{b} - \sum_{j=1}^m \frac{F^{ij} r_i r_j}{ab} \right) \frac{r_i}{b}, S_y = \sum_{j=1}^m \frac{S^j r_j}{a} + \sum_{i=1}^n \left(\frac{S^i r_i}{b} - \sum_{j=1}^m \frac{S^{ij} r_i r_j}{ab} \right) \frac{r_i}{b}. \quad (26)$$

The remaining reduced stiffness properties of the stiffened shell will be as follows:

$$J_x = \sum_{i=1}^n \frac{J^i r_i}{b} + \sum_{j=1}^m \left(\frac{J^j r_j}{a} - \sum_{i=1}^n \frac{J^{ij} r_i r_j}{ab} \right) \frac{r_j}{a}, J_y = \sum_{j=1}^m \frac{J^j r_j}{a} + \sum_{i=1}^n \left(\frac{J^i r_i}{b} - \sum_{j=1}^m \frac{J^{ij} r_i r_j}{ab} \right) \frac{r_i}{b}. \quad (27)$$

For shells of arbitrary form in Eqs. (17)–(19), \tilde{a} should be taken instead of a , and \tilde{b} should be taken instead of b , where $\tilde{a} = aA$, $\tilde{b} = bB$, $B = B(x) = B(a/2)$, then \tilde{a} and \tilde{b} will be measured in meters, and a and b can be measured in radians.

Remaining equations for the forces and moments acting in the layer, equivalent to stiffeners in terms of stiffness, will be as follows:

$$\begin{aligned} M_x^R &= G_1^R [S_x (\varepsilon_x + \mu \varepsilon_y) + J_x (\chi_1 + \mu \chi_2)], \\ M_y^R &= G_2^R [S_y (\varepsilon_y + \mu \varepsilon_x) + J_y (\chi_2 + \mu \chi_1)], \\ N_{xy}^R &= G_{12}^R [F_y \gamma_{xy} + 2S_y \chi_{12}], N_{yx}^R = G_{12}^R [F_x \gamma_{xy} + 2S_x \chi_{12}], \\ M_{xy}^R &= G_{12}^R [S_y \gamma_{xy} + 2J_y \chi_{12}], M_{yx}^R = G_{12}^R [S_x \gamma_{xy} + 2J_x \chi_{12}], \\ Q_x^R &= G_{13}^R F_x k(\Psi_x - \theta_1), \quad Q_y^R = G_{23}^R F_y k(\Psi_y - \theta_2). \end{aligned} \quad (28)$$

In Eqs. (25)–(27), the height of stiffeners can depend on the coordinate along which they are located; i.e. $h^i = h^i(x)$, $h^j = h^j(y)$. In this case, a structurally orthotropic shell is a shell of variable thickness. A concentration of stresses is observed for panels of conical, spherical and toroidal shells near the edge $x = 0$. Introducing stiffeners of variable height can decrease this concentration of stresses.

2.7. Refined model of a stiffened shell with discrete introduction of stiffeners

The model presented in this paragraph is new and has not been published anywhere else by the authors.

The model of a stiffened shell described in Section 2.4 can be refined. The skin is represented by a solid layer with thickness h . Thus, stiffness properties related to the forces and moments of the skin can be found by integrating the stress with respect to z from $-h/2$ to $h/2$. The stiffening layer is discrete, and the stiffness of this layer in the x , y directions can vary. Therefore, stiffness properties related to forces and moments acting in stiffeners (superscript “R”) will not correspond exactly to the area of the cross-section or longitudinal section of stiffeners per unit of section length, the static moment, or the moment of inertia of that section (18).

In the version of the method of structural anisotropy developed by Karpov (Karpov, 2018, Karpov, 2010), when the stiffness of stiffeners perpendicular to the direction under consideration is taken into account, a modular ratio, which is equal to the ratio between the width of the stiffeners in this direction and the linear dimension of the shell in the direction under consideration, is introduced under the summation sign.

Semenov suggested introducing the same modular ratio for stiffness properties when shells are discretely reinforced with stiffeners.

The total stiffness includes that of stiffeners in the direction under consideration and that of stiffeners in the orthogonal direction.

Let us consider forces acting in the direction of the x axis in stiffeners:

$$N_x^R = G_1^R [\bar{F}_x(\varepsilon_x + \mu_{21}\varepsilon_y) + \bar{S}_x(\chi_1 + \mu_{21}\chi_2)]. \quad (29)$$

This force can be represented as follows:

$$N_x^R = N_x^{LR} + N_x^{BR}. \quad (30)$$

Here, LR means that longitudinal stiffeners, i.e. stiffeners parallel to the x axis, are considered.

$$N_x^{LR} = \sum_{i=1}^n G_1^R (F^i(\varepsilon_x + \mu_{21}\varepsilon_y) + S^i(\chi_1 + \mu_{21}\chi_2)) \bar{\delta}(y - y_i) K_{11}. \quad (31)$$

The discreteness of stiffeners parallel to the x axis is defined by unit column function $\bar{\delta}(y - y_i)$, and these stiffeners are located along the entire shell, i.e. from $x = 0$ to $x = a$. That is why multiplier $K_{11} = a/a$.

Superscript BR means that stiffeners perpendicular to the x axis are considered.

$$N_x^{BR} = \sum_{j=1}^m [G_1^R (F^j(\varepsilon_x + \mu_{21}\varepsilon_y) + S^j(\chi_1 + \mu_{21}\chi_2)) \bar{\delta}(x - x_j) K_{12} - \sum_{i=1}^n G_1^R (F^{ij}(\varepsilon_x + \mu_{21}\varepsilon_y) + S^{ij}(\chi_1 + \mu_{21}\chi_2)) \bar{\delta}(y - y_i) \bar{\delta}(x - x_j) K_{12}]. \quad (32)$$

The discreteness of stiffeners perpendicular to the x axis is defined by unit column function $\bar{\delta}(x - x_j)$. Transverse stiffeners of width r_j/a are located not all along the x axis, but discretely, and N_x^{BR} at $x = a_j$, $x = b_j$ equals 0 (Karpov, 1999). Thus, multiplier $K_{12} = r_j/(aA)$.

The second multiplier in the N_x^{BR} equation corresponds to the common portion of intersecting stiffeners (this part was already included in the N_x^{LR} equation, and should therefore be subtracted). Finally, for N_x^R , we derive the following:

$$N_x^R = G_1^R \left[\sum_{i=1}^n (F^i(\varepsilon_x + \mu_{21}\varepsilon_y) + S^i(\chi_1 + \mu_{21}\chi_2)) \bar{\delta}(y - y_i) + \sum_{j=1}^m (F^j(\varepsilon_x + \mu_{21}\varepsilon_y) + S^j(\chi_1 + \mu_{21}\chi_2)) \bar{\delta}(x - x_j) \frac{r_j}{aA} - \sum_{j=1}^m \sum_{i=1}^n (F^{ij}(\varepsilon_x + \mu_{21}\varepsilon_y) + S^{ij}(\chi_1 + \mu_{21}\chi_2)) \bar{\delta}(y - y_i) \bar{\delta}(x - x_j) \frac{r_j}{aA} \right] \quad (33)$$

or in a more compact form:

$$N_x^R = G_1^R [\bar{F}_x(\varepsilon_x + \mu_{21}\varepsilon_y) + \bar{S}_x(\chi_1 + \mu_{21}\chi_2)], \quad (34)$$

where:

$$\bar{F}_x = \sum_{i=1}^n F^i \bar{\delta}(y - y_i) + r_a \left[\sum_{j=1}^m F^j \bar{\delta}(x - x_j) - \sum_{i=1}^n \sum_{j=1}^m F^{ij} \bar{\delta}(x - x_j) \bar{\delta}(y - y_i) \right], \quad (35)$$

$$\bar{S}_x = \sum_{i=1}^n S^i \bar{\delta}(y - y_i) + r_a \left[\sum_{j=1}^m S^j \bar{\delta}(x - x_j) - \sum_{i=1}^n \sum_{j=1}^m S^{ij} \bar{\delta}(x - x_j) \bar{\delta}(y - y_i) \right],$$

The remaining forces and moments acting in stiffeners can be presented as follows:

$$M_x^R = G_1^R [\bar{S}_x(\varepsilon_x + \mu_{21}\varepsilon_y) + \bar{J}_x(\chi_1 + \mu_{21}\chi_2)],$$

$$N_y^R = G_2^R [\bar{F}_y(\varepsilon_y + \mu_{12}\varepsilon_x) + \bar{S}_y(\chi_2 + \mu_{12}\chi_1)], \quad M_y^R = G_2^R [\bar{S}_y(\varepsilon_y + \mu_{12}\varepsilon_x) + \bar{J}_y(\chi_2 + \mu_{12}\chi_1)],$$

$$N_{xy}^R = G_{12}^R [\bar{F}_{xy}\gamma_{xy} + 2\bar{S}_{xy}\chi_{12}], \quad M_{xy}^R = G_{12}^R [\bar{S}_{xy}\gamma_{xy} + \bar{J}_{xy}\chi_{12}],$$

$$Q_x^R = G_{13}^R k \bar{F}_x(\Psi_x - \theta_1), \quad Q_y^R = G_{23}^R k \bar{F}_y(\Psi_y - \theta_2). \quad (36)$$

Here, in addition to (35):

$$\begin{aligned}\bar{F}_y &= \sum_{j=1}^m F^j \bar{\delta}(x - x_j) + r_b \left[\sum_{i=1}^n F^i \bar{\delta}(y - y_i) - \sum_{i=1}^n \sum_{j=1}^m F^{ij} \bar{\delta}(x - x_j) \bar{\delta}(y - y_i) \right], \\ \bar{S}_y &= \sum_{j=1}^m S^j \bar{\delta}(x - x_j) + r_b \left[\sum_{i=1}^n S^i \bar{\delta}(y - y_i) - \sum_{i=1}^n \sum_{j=1}^m S^{ij} \bar{\delta}(x - x_j) \bar{\delta}(y - y_i) \right], \\ \bar{J}_x &= \sum_{i=1}^n J^i \bar{\delta}(y - y_i) + r_a \left[\sum_{j=1}^m J^j \bar{\delta}(x - x_j) - \sum_{i=1}^n \sum_{j=1}^m J^{ij} \bar{\delta}(x - x_j) \bar{\delta}(y - y_i) \right], \\ \bar{J}_y &= \sum_{j=1}^m J^j \bar{\delta}(x - x_j) + r_b \left[\sum_{i=1}^n J^i \bar{\delta}(y - y_i) - \sum_{i=1}^n \sum_{j=1}^m J^{ij} \bar{\delta}(x - x_j) \bar{\delta}(y - y_i) \right],\end{aligned}\quad (37)$$

$$\begin{aligned}\bar{F}_{xy} &= \frac{1}{2} (\bar{F}_x + \bar{F}_y) = \frac{1}{2} \sum_{i=1}^n F^i (1 + r_b) \bar{\delta}(y - y_i) + \frac{1}{2} \sum_{j=1}^m F^j (1 + r_a) \bar{\delta}(x - x_j) \\ &\quad - \sum_{i=1}^n \sum_{j=1}^m F^{ij} r_{ab} \bar{\delta}(x - x_j) \bar{\delta}(y - y_i), \\ \bar{S}_{xy} &= \frac{1}{2} (\bar{S}_x + \bar{S}_y) = \frac{1}{2} \sum_{i=1}^n S^i (1 + r_b) \bar{\delta}(y - y_i) + \frac{1}{2} \sum_{j=1}^m S^j (1 + r_a) \bar{\delta}(x - x_j) \\ &\quad - \sum_{i=1}^n \sum_{j=1}^m S^{ij} r_{ab} \bar{\delta}(x - x_j) \bar{\delta}(y - y_i), \\ \bar{J}_{xy} &= \frac{1}{2} (\bar{J}_x + \bar{J}_y) = \frac{1}{2} \sum_{i=1}^n J^i (1 + r_b) \bar{\delta}(y - y_i) + \frac{1}{2} \sum_{j=1}^m J^j (1 + r_a) \bar{\delta}(x - x_j) \\ &\quad - \sum_{i=1}^n \sum_{j=1}^m J^{ij} r_{ab} \bar{\delta}(x - x_j) \bar{\delta}(y - y_i),\end{aligned}$$

where:

$$r_a = \frac{r_j}{aA}, \quad r_b = \frac{r_i}{bB}, \quad r_{ab} = \frac{r_a + r_b}{2}.$$

3. Methods

3.1. Transformation of the functional

3.1.1. Transformation of the functional for a stiffened shell in contact with the skin along a line

If stiffeners are introduced using delta functions (10), the functional E_s^R will be as follows:

$$\begin{aligned}E_s^R &= \frac{1}{2} \int_{a_1}^a \int_0^b \left[N_x^R \varepsilon_x + N_y^R \varepsilon_y + M_x^R \chi_1 + M_y^R \chi_2 \right] AB dx dy = \\ &= \frac{1}{2} \int_{a_1}^a \int_0^b \left[E_1 \sum_{i=1}^n \left(F^i r_i \varepsilon_x^2 + S^i r_i \chi_1 \varepsilon_x \right) \delta(y - y_i) + E_2 \sum_{j=1}^m \left(F^j r_j \varepsilon_y^2 + S^j r_j \chi_2 \varepsilon_y \right) \delta(x - x_j) \right. \\ &\quad \left. + E_1 \sum_{i=1}^n \left(S^i r_i \varepsilon_x \chi_1 + J^i r_i \chi_1^2 \right) \delta(y - y_i) + E_2 \sum_{j=1}^m \left(S^j r_j \varepsilon_y \chi_2 + J^j r_j \chi_2^2 \right) \delta(x - x_j) \right] AB dx dy.\end{aligned}\quad (38)$$

Let us write this equation in the following form:

$$E_s^R = \frac{1}{2} \int_{a_1}^a \int_0^b \left[\sum_{i=1}^n A_{1i} \delta(y - y_i) + \sum_{j=1}^m A_{2j} \delta(x - x_j) \right] dx dy, \quad (39)$$

where:

$$\begin{aligned}A_{1i} &= E_1 \left(F^i r_i \varepsilon_x^2 + S^i r_i \chi_1 \varepsilon_x + S^i r_i \chi_1 \varepsilon_x + J^i r_i \chi_1^2 \right) AB, \\ A_{2j} &= E_2 \left(F^j r_j \varepsilon_y^2 + S^j r_j \chi_2 \varepsilon_y + S^j r_j \chi_2 \varepsilon_y + J^j r_j \chi_2^2 \right) AB.\end{aligned}\quad (40)$$

Therefore:

$$E_s^R = \frac{1}{2} \int_{a_1}^a \sum_{i=1}^n \left(A_{1i} \Big|_{y=y_i} \right) dx + \frac{1}{2} \int_0^b \sum_{j=1}^m \left(A_{2j} \Big|_{x=x_j} \right) dy. \quad (41)$$

3.1.2. Transformation of the functional for a stiffened shell in contact with the skin along a strip

Let us apply the equations for forces and moments (18) to functional (8):

$$\begin{aligned}
 E_s^R = & \frac{1}{2} \int_{a_1}^a \int_0^b \left[G_1^R [\bar{F}(\varepsilon_x + \mu_{21}\varepsilon_y) + \bar{S}(\chi_1 + \mu_{21}\chi_2)] \varepsilon_x + G_2^R [\bar{F}(\varepsilon_y + \mu_{12}\varepsilon_x) + \bar{S}(\chi_2 + \mu_{12}\chi_1)] \varepsilon_y \right. \\
 & + \frac{1}{2} (G_{12}^R [\bar{F}\gamma_{xy} + 2\bar{S}\chi_{12}] + G_{12}^R [\bar{F}\gamma_{xy} + 2\bar{S}\chi_{12}]) \gamma_{xy} + G_1^R [\bar{S}(\varepsilon_x + \mu_{21}\varepsilon_y) + \bar{J}(\chi_1 + \mu_{21}\chi_2)] \chi_1 \\
 & + G_2^R [\bar{S}(\varepsilon_y + \mu_{12}\varepsilon_x) + \bar{J}(\chi_2 + \mu_{12}\chi_1)] \chi_2 + (G_{12}^R [\bar{S}\gamma_{xy} + 2\bar{J}\chi_{12}] + G_{12}^R [\bar{S}\gamma_{xy} + 2\bar{J}\chi_{12}]) \chi_{12} \\
 & + G_{13}^R k \bar{F}(\Psi_x - \theta_1)(\Psi_x - \theta_1) + G_{23}^R k \bar{F}(\Psi_y - \theta_2)(\Psi_y - \theta_2) \Big] AB dx dy = \\
 = & \frac{1}{2} \int_{a_1}^a \int_0^b \left[\bar{F} [G_1^R(\varepsilon_x + \mu_{21}\varepsilon_y)\varepsilon_x + G_2^R(\varepsilon_y + \mu_{12}\varepsilon_x)\varepsilon_y + G_{12}^R \gamma_{xy}^2 + G_{13}^R k(\Psi_x - \theta_1)^2 \right. \\
 & + G_{23}^R k(\Psi_y - \theta_2)^2] + \bar{S} [G_1^R(\chi_1 + \mu_{21}\chi_2)\varepsilon_x + G_2^R(\chi_2 + \mu_{12}\chi_1)\varepsilon_y \\
 & + G_1^R(\varepsilon_x + \mu_{21}\varepsilon_y)\chi_1 + G_2^R(\varepsilon_y + \mu_{12}\varepsilon_x)\chi_2 + 4G_{12}^R \gamma_{xy}\chi_{12}] + \bar{J} [G_1^R(\chi_1 + \mu_{21}\chi_2)\chi_1 \\
 & + G_2^R(\chi_2 + \mu_{12}\chi_1)\chi_2 + 4G_{12}^R \chi_{12}^2] \Big] AB dx dy.
 \end{aligned} \quad (42)$$

When Eqs. (16) and (17) are used, we obtain the following:

$$E_s^R = \frac{1}{2} \int_{a_1}^a \int_0^b \left[\sum_{i=1}^n A_{1i} \bar{\delta}(y - y_i) + \sum_{j=1}^m A_{2j} \bar{\delta}(x - x_j) - \sum_{i=1}^n \sum_{j=1}^m A_{3ij} \bar{\delta}(x - x_j) \bar{\delta}(y - y_i) \right] dx dy, \quad (43)$$

where:

$$\begin{aligned}
 A_{1i} = & \left[F^i (G_1^R(\varepsilon_x + \mu_{21}\varepsilon_y)\varepsilon_x + G_2^R(\varepsilon_y + \mu_{12}\varepsilon_x)\varepsilon_y + G_{12}^R \gamma_{xy}^2 + G_{13}^R k(\Psi_x - \theta_1)^2 + G_{23}^R k(\Psi_y - \theta_2)^2) \right. \\
 & + S^i (G_1^R(\chi_1 + \mu_{21}\chi_2)\varepsilon_x + G_2^R(\chi_2 + \mu_{12}\chi_1)\varepsilon_y + G_1^R(\varepsilon_x + \mu_{21}\varepsilon_y)\chi_1 + G_2^R(\varepsilon_y + \mu_{12}\varepsilon_x)\chi_2 + 4G_{12}^R \chi_{12}\gamma_{xy}) \\
 & + J^i (G_1^R(\chi_1 + \mu_{21}\chi_2)\chi_1 + G_2^R(\chi_2 + \mu_{12}\chi_1)\chi_2 + 4G_{12}^R \chi_{12}^2) \Big] AB, \\
 A_{2j} = & \left[F^j (G_1^R(\varepsilon_x + \mu_{21}\varepsilon_y)\varepsilon_x + G_2^R(\varepsilon_y + \mu_{12}\varepsilon_x)\varepsilon_y + G_{12}^R \gamma_{xy}^2 + G_{13}^R k(\Psi_x - \theta_1)^2 + G_{23}^R k(\Psi_y - \theta_2)^2) \right. \\
 & + S^j (G_1^R(\chi_1 + \mu_{21}\chi_2)\varepsilon_x + G_2^R(\chi_2 + \mu_{12}\chi_1)\varepsilon_y + G_1^R(\varepsilon_x + \mu_{21}\varepsilon_y)\chi_1 + G_2^R(\varepsilon_y + \mu_{12}\varepsilon_x)\chi_2 + 4G_{12}^R \chi_{12}\gamma_{xy}) \\
 & + J^j (G_1^R(\chi_1 + \mu_{21}\chi_2)\chi_1 + G_2^R(\chi_2 + \mu_{12}\chi_1)\chi_2 + 4G_{12}^R \chi_{12}^2) \Big] AB, \\
 A_{3ij} = & \left[F^{ij} (G_1^R(\varepsilon_x + \mu_{21}\varepsilon_y)\varepsilon_x + G_2^R(\varepsilon_y + \mu_{12}\varepsilon_x)\varepsilon_y + G_{12}^R \gamma_{xy}^2 + G_{13}^R k(\Psi_x - \theta_1)^2 + G_{23}^R k(\Psi_y - \theta_2)^2) \right. \\
 & + S^{ij} (G_1^R(\chi_1 + \mu_{21}\chi_2)\varepsilon_x + G_2^R(\chi_2 + \mu_{12}\chi_1)\varepsilon_y + G_1^R(\varepsilon_x + \mu_{21}\varepsilon_y)\chi_1 + G_2^R(\varepsilon_y + \mu_{12}\varepsilon_x)\chi_2 + 4G_{12}^R \chi_{12}\gamma_{xy}) \\
 & + J^{ij} (G_1^R(\chi_1 + \mu_{21}\chi_2)\chi_1 + G_2^R(\chi_2 + \mu_{12}\chi_1)\chi_2 + 4G_{12}^R \chi_{12}^2) \Big] AB.
 \end{aligned}$$

The functional (43) can be written as follows:

$$E_s^R = \frac{1}{2} \int_{a_1}^a dx \sum_{i=1}^n \int_{c_i}^{d_i} A_{1i} dy + \frac{1}{2} \int_0^b dy \sum_{j=1}^m \int_{a_j}^{b_j} A_{2j} dx - \sum_{i=1}^n \sum_{j=1}^m \int_{a_j}^{b_j} \int_{c_i}^{d_i} A_{3ij} dx dy. \quad (44)$$

3.1.3. Transformation of the functional for a stiffened shell with "smearing" of the stiffness of stiffeners using the method of structural anisotropy

Let us apply the equations for forces and moments (28) to functional (8)

$$\begin{aligned}
 E_s^R = & \frac{1}{2} \int_{a_1}^a \int_0^b \left[F_x (G_1^R(\varepsilon_x + \mu\varepsilon_y)\varepsilon_x + \frac{1}{2} G_{12}^R \gamma_{xy}^2 + G_{13}^R k(\Psi_x - \theta_1)^2) \right. \\
 & + F_y (\frac{1}{2} G_{12}^R \gamma_{xy}^2 + G_2^R(\varepsilon_y + \mu\varepsilon_x)\varepsilon_y + G_{23}^R k(\Psi_y - \theta_2)^2) \\
 & + S_y (2G_{12}^R \chi_{12}\gamma_{xy} + G_2^R(\chi_2 + \mu\chi_1)\varepsilon_y + G_2^R(\varepsilon_y + \mu\varepsilon_x)\chi_2) \\
 & + S_x (2G_{12}^R \chi_{12}\gamma_{xy} + G_1^R(\chi_1 + \mu\chi_2)\varepsilon_x + G_1^R(\varepsilon_x + \mu\varepsilon_y)\chi_1) \\
 & + J_y (2G_{12}^R \chi_{12}\chi_{12} + G_2^R(\chi_2 + \mu\chi_1)\chi_2) + J_x (G_1^R(\chi_1 + \mu\chi_2)\chi_1 + 2G_{12}^R \chi_{12}^2) \Big] AB dx dy
 \end{aligned} \quad (45)$$

3.1.4. Transformation of the functional for a stiffened shell using the refined version of the model

Let us break functional (7) into two parts due to the fact that in, the second integral, we will calculate both the integrals over sections $[0, a]$, $[0, b]$, and the sums of the integrals over sections $[a_j, b_j]$, $[c_i, d_i]$.

The double integral is converted into iterated integrals, and then Simpson's rule is applied. The integral with respect to x is the outer integral, because, at each value of x , the integral with respect to y is calculated first, as it includes a member that depends on x ($r_b = \frac{r_i}{bB(x)}$).

When the equations of forces and moments are applied to (8), we obtain the following:

$$E_s^R = \frac{1}{2} \int_{a_1}^a \int_0^b \left[\sum_{j=1}^m A_{1j} \bar{\delta}(x - x_j) + \sum_{i=1}^n A_{2i} \bar{\delta}(y - y_i) - \sum_{i=1}^n \sum_{j=1}^m A_{3ij} \bar{\delta}(x - x_j) \bar{\delta}(y - y_i) \right] dx dy. \quad (46)$$

Table 1
Geometrical parameters of shells.

No.	$a = b$, m	$R_1 = R_2$, m	h , m
1	54	135.9	0.09
2	18	45.27	0.09
3	10.8	40.05	0.09

Here:

$$\begin{aligned}
 A_{1j} &= [G_1^R(F^j \hat{\varepsilon}_x \varepsilon_x + S^j \hat{\chi}_1 \varepsilon_x) r_a + G_2^R(F^j \hat{\varepsilon}_y \varepsilon_y + S^j \hat{\chi}_2 \varepsilon_y) \\
 &+ \frac{1}{2} G_{12}^R(F^j \gamma_{xy}^2 + 2S^j \chi_{12} \gamma_{xy})(1 + r_a) + G_1^R(S^j \hat{\varepsilon}_x \chi_1 + J^j \hat{\chi}_1 \chi_1) r_a \\
 &+ G_2^R(S^j \hat{\varepsilon}_y \chi_2 + J^j \hat{\chi}_2 \chi_2) + G_{12}^R(S^j \gamma_{xy} \chi_{12} + 2J^j \chi_{12}^2)(1 + r_a) + \hat{\Psi}_x F^j r_a + \hat{\Psi}_y F^j] AB, \\
 A_{2i} &= [G_1^R(F^i \hat{\varepsilon}_x \varepsilon_x + S^i \hat{\chi}_1 \varepsilon_x) + G_2^R(F^i \hat{\varepsilon}_y \varepsilon_y + S^i \hat{\chi}_2 \varepsilon_y) r_b \\
 &+ \frac{1}{2} G_{12}^R(F^i \gamma_{xy}^2 + 2S^i \chi_{12} \gamma_{xy})(1 + r_b) + G_1^R(S^i \hat{\varepsilon}_x \chi_1 + J^i \hat{\chi}_1 \chi_1) \\
 &+ G_2^R(S^i \hat{\varepsilon}_y \chi_2 + J^i \hat{\chi}_2 \chi_2) r_b + G_{12}^R(S^i \gamma_{xy} \chi_{12} + 2J^i \chi_{12}^2)(1 + r_b) + \hat{\Psi}_x F^i + \hat{\Psi}_y F^i r_b] AB, \\
 A_{3ij} &= [G_1^R(F^{ij} \hat{\varepsilon}_x \varepsilon_x + S^{ij} \hat{\chi}_1 \varepsilon_x) r_a + G_2^R(F^{ij} \hat{\varepsilon}_y \varepsilon_y + S^{ij} \hat{\chi}_2 \varepsilon_y) r_b + G_{12}^R(F^{ij} \gamma_{xy}^2 + 2S^{ij} \chi_{12} \gamma_{xy}) r_{ab} \\
 &+ G_1^R(S^{ij} \hat{\varepsilon}_x \chi_1 + J^{ij} \hat{\chi}_1 \chi_1) r_a + G_2^R(S^{ij} \hat{\varepsilon}_y \chi_2 + J^{ij} \hat{\chi}_2 \chi_2) r_b \\
 &+ 2G_{12}^R(S^{ij} \gamma_{xy} \chi_{12} + 2J^{ij} \chi_{12}^2) r_{ab} + \hat{\Psi}_x F^{ij} r_a + \hat{\Psi}_y F^{ij} r_b] AB,
 \end{aligned} \tag{47}$$

where, for a more concise form, the notation is introduced:

$$\hat{\varepsilon}_x = (\varepsilon_x + \mu_{21} \varepsilon_y), \quad \hat{\varepsilon}_y = (\varepsilon_y + \mu_{12} \varepsilon_x), \quad \hat{\chi}_1 = (\chi_1 + \mu_{21} \chi_2), \quad \hat{\chi}_2 = (\chi_2 + \mu_{12} \chi_1),$$

$$\hat{\Psi}_x = G_{13}^R k (\Psi_x - \theta_1)^2, \quad \hat{\Psi}_y = G_{23}^R k (\Psi_y - \theta_2)^2.$$

Functional (46) can be written as follows:

$$E_s^R = \frac{1}{2} \int_0^b dy \sum_{j=1}^m \int_{a_j}^{b_j} A_{1j} dx + \frac{1}{2} \int_{a_1}^a dx \sum_{i=1}^n \int_{c_i}^{d_i} A_{2i} dy - \sum_{i=1}^n \sum_{j=1}^m \int_{a_j}^{b_j} \int_{c_i}^{d_i} A_{3ij} dx dy. \tag{48}$$

3.2. Ritz method

This paper suggests using an algorithm based on the Ritz method and the best parameter continuation method for studying shell structures.

According to this algorithm, the Ritz method is applied to the functional to reduce the variational problem to a system of nonlinear algebraic equations. For this purpose, the required functions are presented as follows:

$$\begin{aligned}
 U &= U(x, y) = \sum_{k=1}^{\sqrt{N}} \sum_{l=1}^{\sqrt{N}} U_{kl} X_1^k Y_1^l, & V &= V(x, y) = \sum_{k=1}^{\sqrt{N}} \sum_{l=1}^{\sqrt{N}} V_{kl} X_2^k Y_2^l, \\
 W &= W(x, y) = \sum_{k=1}^{\sqrt{N}} \sum_{l=1}^{\sqrt{N}} W_{kl} X_3^k Y_3^l, \\
 \Psi_x &= \Psi_x(x, y) = \sum_{k=1}^{\sqrt{N}} \sum_{l=1}^{\sqrt{N}} P S_{kl} X_4^k Y_4^l, & \Psi_y &= \Psi_y(x, y) = \sum_{k=1}^{\sqrt{N}} \sum_{l=1}^{\sqrt{N}} P N_{kl} X_5^k Y_5^l,
 \end{aligned} \tag{49}$$

where $U_{kl} - PN_{kl}$ are unknown numerical parameters. Having applied functions (49) to functional (7), we find the derivatives with respect to unknown numerical parameters $U_{kl} - PN_{kl}$. Thus, we derive a system of nonlinear algebraic equations.

To solve this system, we can apply the method of successive loadings (Petrov, 1975) with a modification (Karpov and Petrov, 1975) that improves the accuracy of the solution, the best parameter continuation method (Kuznetsov, 2012, Karpov and Semenov, 2017), or the iterative method (Karpov, 2011). The results presented in this paper were derived using the best parameter continuation method.

Verification of this algorithm is considered in detail in (Semenov, 2016).

All calculations are performed using dimensionless parameters. However, the reasoning uses dimensions to avoid unnecessary complexity of the equations. The dimensionless parameters and their justification are given in detail in (Karpov and Semenov, 2018).

Table 2
Buckling load values for a structure of version 1.

Number of stiffeners		q_{cr} , MPa					
		0×0	4×4	8×8	12×12	16×16	20×20
$N=9$	Discrete introduction of stiffeners along a line (Lurie, 1948) (Lurie, 1948)	0,1133	0,1517	0,1771	0,1810	0,1864	0,1916
	Discrete introduction of stiffeners along a strip (Karpov, 1986) (Ilyin and Karpov, 1986, Karpov, 2018)		0,1998	0,2279	0,2547	0,2787	0,3010
	Structural anisotropy method (Karpov, 2010) (Karpov, 2018, Karpov, 2010)		0,1654	0,1984	0,2143	0,2292	0,2433
	Refined discrete introduction of stiffeners along a strip (Semenov)		0,1574	0,1977	0,2142	0,2292	0,2432
$N=16$	Discrete introduction of stiffeners along a line (Lurie, 1948) (Lurie, 1948)	0,0957	0,1226	0,1345	0,1484	0,1597	0,1689
	Discrete introduction of stiffeners along a strip (Karpov, 1986) (Ilyin and Karpov, 1986, Karpov, 2018)		0,1597	0,2041	0,2343	0,2616	0,2859
	Structural anisotropy method (Karpov, 2010) (Karpov, 2018, Karpov, 2010)		0,1328	0,1606	0,1835	0,2031	0,2204
	Refined discrete introduction of stiffeners along a strip (Semenov)		0,1316	0,1643	0,1838	0,2033	0,2206

Table 3
Buckling load values for shells of versions 2 and 3.

Number of stiffeners		q_{cr} , MPa					
		0×0	4×4	8×8	12×12	16×16	20×20
$N=9$	Version 2	0,6862	1,1118	2,5409	3,0602	3,4800	3,8374
	Version 3	0,8159	2,0123	2,4863	–	–	–
$N=16$	Version 2	0,6238	1,1410	2,5078	3,0508	3,4762	3,8370
	Version 3	0,8023	1,8695	2,4812	–	–	–

Table 4
Buckling loads for the version of the structure tested in experiments.

Number of stiffeners		q_{cr} , MPa 9×9
Experimental data (Klimanov and Timashev, 1985) (Klimanov and Timashev, 1985)		$0.503 \cdot 10^{-2}$
$N=16$	Discrete introduction of stiffeners along a line (Lurie, 1948) (Lurie, 1948)	$0.350 \cdot 10^{-2}$
	Discrete introduction of stiffeners along a strip (Karpov, 1986) (Ilyin and Karpov, 1986, Karpov, 2018)	$0.733 \cdot 10^{-2}$
	Structural anisotropy method (Karpov, 2010) (Karpov, 2018, Karpov, 2010)	$0.537 \cdot 10^{-2}$
	Refined discrete introduction of stiffeners along a strip (Semenov)	$0.551 \cdot 10^{-2}$

4. Analysis

Let us demonstrate the applicability of the above methods for introducing stiffeners using an example of analyzing shallow doubly curved shells made of an isotropic material (steel with parameters $E = 2.1 \cdot 10^5$ MPa, $\mu = 0.3$). The shells are square, with fixed pin joints along the contour, and under uniformly distributed transverse load q directed normal to the surface.

In this case, the following approximation is used:

$$U = U(x, y) = \sum_{k=1}^{\sqrt{N}} \sum_{l=1}^{\sqrt{N}} U_{kl} \sin \left(2k\pi \frac{x}{a} \right) \sin \left((2l-1)\pi \frac{y}{b} \right),$$

$$V = V(x, y) = \sum_{k=1}^{\sqrt{N}} \sum_{l=1}^{\sqrt{N}} V_{kl} \sin \left((2k-1)\pi \frac{x}{a} \right) \sin \left(2l\pi \frac{y}{b} \right),$$

$$W = W(x, y) = \sum_{k=1}^{\sqrt{N}} \sum_{l=1}^{\sqrt{N}} W_{kl} \sin \left((2k-1)\pi \frac{x}{a} \right) \sin \left((2l-1)\pi \frac{y}{b} \right),$$

$$\Psi_x = \Psi_x(x, y) = \sum_{k=1}^{\sqrt{N}} \sum_{l=1}^{\sqrt{N}} \Psi_{xkl} \cos \left((2k-1)\pi \frac{x}{a} \right) \sin \left((2l-1)\pi \frac{y}{b} \right),$$

$$\Psi_y = \Psi_y(x, y) = \sum_{k=1}^{\sqrt{N}} \sum_{l=1}^{\sqrt{N}} \Psi_{ykl} \sin \left((2k-1)\pi \frac{x}{a} \right) \cos \left((2l-1)\pi \frac{y}{b} \right), \quad (50)$$

The shells are reinforced with an orthogonal grid of stiffeners uniformly distributed throughout the structure. The width of the stiffeners is $r^j = r^i = 2h$, and the height is $h^j = h^i = 3h$. Let us define the distance between the stiffeners as x_r . The outer stiffeners will be at a distance $0.5x_r$ from the edge of the structure.

Geometrical parameters of shells are given in Table 1.

Using the Ritz method, let us set $N = 9$ and $N = 16$. The method's convergence was considered in more detail in (Karpov, 2011).

Let us consider all three methods for the discrete introduction of stiffeners using a structure of version 1 as an example. Table 2 shows the resulting buckling load values q_{cr} when a significant change in the structure's deflection corresponds to a small change in load.

Fig. 2 presents the Table 2 data in graphic form.

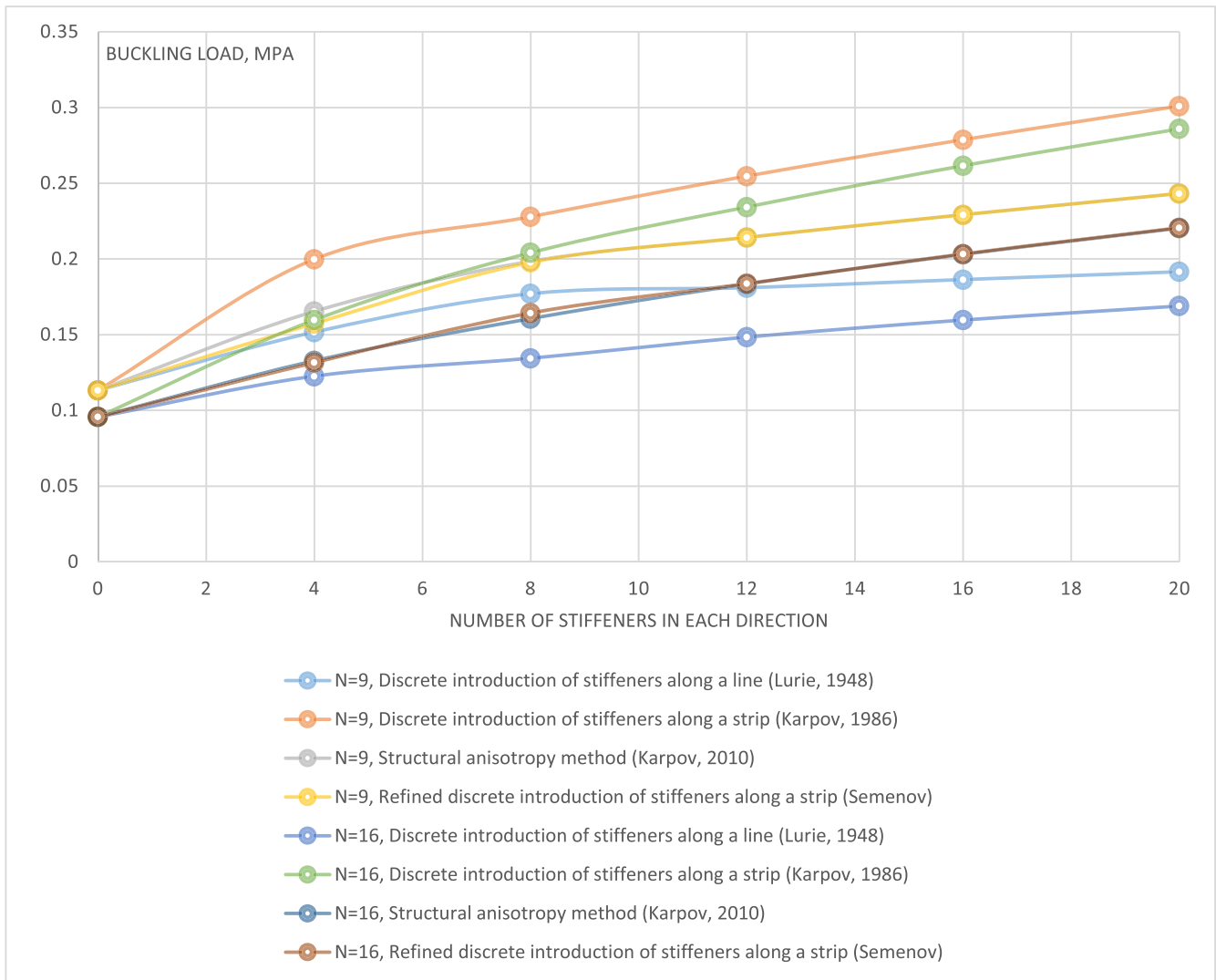


Fig. 2. Analysis results for a structure of version 1 using various models.

Fig. 3 shows a load-deflection graph for various methods of calculating the stiffening of the shell under consideration with a 16×16 grid of stiffeners and $N = 16$ (curves W_c – deflection in the center of the structure; curves W_4 – deflection in a quarter of the structure; the superscript indicates the method for calculating the stiffeners). As it is evident from the data presented for this structure, in addition to the general buckling, there is also local buckling at a load of about 0.2 MPa. There is a significant difference in the values of the deflections in the center and in the quarter of the structure, as well as the formation of a “loop” in the graph.

Fig. 4 shows a load-deflection graph, with various numbers of stiffeners and calculations using the more accurate approach suggested in this paper (brown curves W_8 – deflection in an eighth of the structure; the superscript indicates the number of stiffeners in each direction). So that the curves remain uncluttered, the figure shows a fragment of the graph before the first case of stability loss.

The data presented show that the discrete introduction of stiffeners along a strip without consideration of adjusting factors results in overestimated values of the critical load, while the approach used by Lurie (when stiffeners are introduced along a line) results in significantly understated values. The refined approach, as

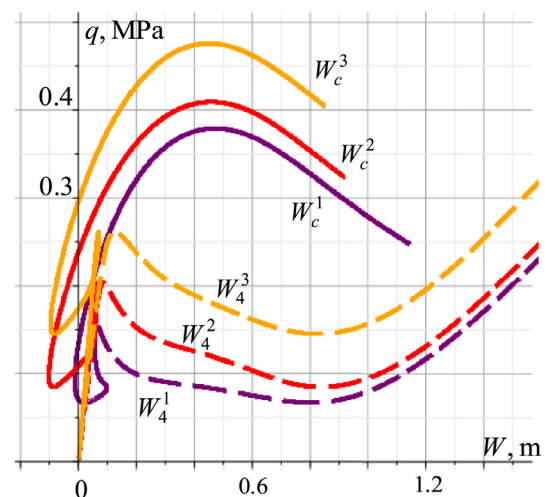


Fig. 3. Load-deflection graph for various methods of calculating the stiffening of the shell under consideration with a 16×16 grid of stiffeners (superscript 1 – introduction of stiffeners along a line (Lurie), superscript 2 – refined introduction of stiffeners along a strip (Semenov), superscript 3 – introduction of stiffeners along a strip (Karpov)).

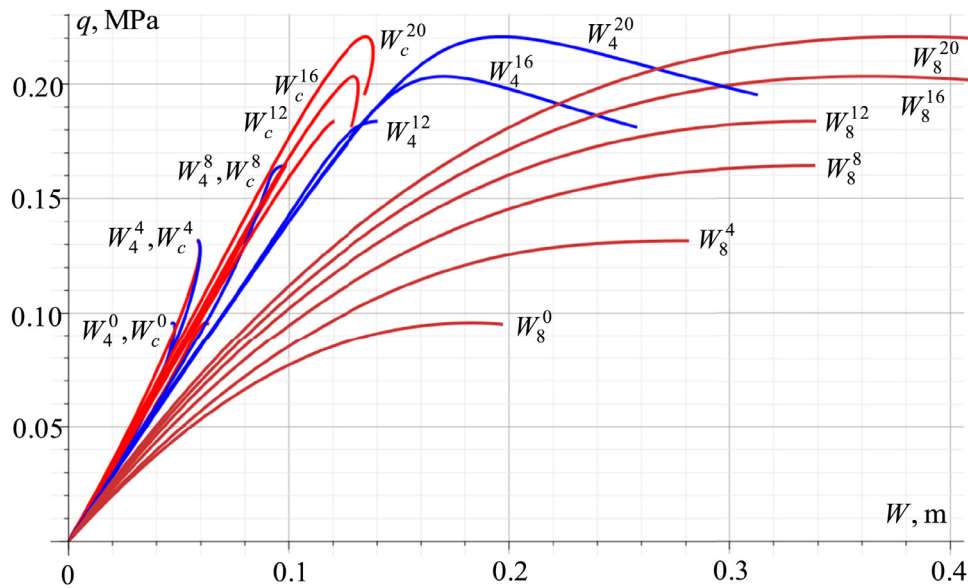


Fig. 4. Load-deflection graph, with various numbers of stiffeners and their calculation using the refined approach suggested in this paper.

well as the method of structural anisotropy, have very close results, and the convergence increases with the number of stiffeners.

Table 3 provides the resulting buckling load values for various stiffening versions of shells of versions 2 and 3 (using the refined approach to introducing stiffeners).

5. Comparison with the experiment

In their publication, Klimanov and Timashev (Klimanov and Timashev, 1985) present results of experiments conducted at the Ural Research Center of the USSR Academy of Sciences to study the buckling of plexiglass shells. The authors tested 18 samples of square shallow doubly curved shells with parameters $h = 0.001$ m, $a = b = 0.604$ m, $R_1 = R_2 = 1.51$ m (material: plexiglass with parameters $E = 0.0331 \cdot 10^5$ MPa, $\mu = 0.354$; parameters of stiffeners: $n = m = 9$, $h^i = h^j = 0.0033$ m, $r = 0.0092$ m). The resulting buckling load values q_{cr} ranged from $0.411 \cdot 10^{-2}$ MPa to $0.703 \cdot 10^{-2}$ MPa. After mathematical processing of the experimental data, the resultant value of the critical load was calculated to be $q_{cr} = 0.503 \cdot 10^{-2}$ MPa.

Analysis for this version of the structure using the methods described in this paper yielded the results given in Table 4.

It is evident from the data obtained that among the discrete methods for introducing stiffeners, the method proposed in this work gives the values closest to the experimental data. The method of structural anisotropy also gives a close value of the critical buckling load. When using discrete introduction of stiffeners along a line, the value of the critical load is significantly underestimated, and when using discrete introduction of stiffeners along a strip, it is significantly overestimated.

Conclusion

Therefore, a mathematical model of the deformation of stiffened shell structures that accounts for geometric nonlinearity and transverse shears is derived. The proposed model may be used to analyze the deformation process of shallow shells of double curvature, cylindrical, conical, spherical, toroidal panels, etc.

In addition, the most accurate account for the work of the ribs during deformation is important; this is achieved in that the contact between the coating and the ribs should be along a strip, rather than a line, and the shear and the torsional rigidity of the

ribs should especially be taken into account. The authors suggest a new, most accurate version to account for stiffness properties of stiffeners, based on introducing various modular ratios along various coordinate axes. For stiffeners perpendicular to the direction under consideration, the authors introduce a modular ratio equal to the ratio between the width of stiffeners in this direction and the linear dimension of the shell in the direction under consideration.

Critical buckling loads were obtained for shallow shells of double curvature; general and local buckling were identified.

Thus, we analyzed approaches to introducing stiffeners for thin-walled shell structures. Analysis results showed that the proposed refined method for calculating stiffness properties is the most accurate. The results also show that, with a sufficiently large number of stiffeners, the method of structural anisotropy provides a result close to the solution obtained using this method.

Declaration of Competing Interest

The authors declare that they have no known competing financial interests or personal relationships that could have appeared to influence the work reported in this paper.

Acknowledgments

The research was supported by RSF (project No. 18-19-00474).

References

- Abramovich, H., Zarutskii, V.A., 2008. Stability and vibrations of nonclosed circular cylindrical shells reinforced with discrete longitudinal ribs. *Int. Appl. Mech.* 44 (1), 16–22. doi:10.1007/s10778-008-0016-3.
- Abramovich, H., Zarutskii, V.A., 2010. Stability and vibrations of cylindrical shells discretely reinforced with rings. *Int. Appl. Mech.* 46 (1), 46–53. doi:10.1007/s10778-010-0280-x.
- Bai, X., Xu, W., Ren, H., Li, J., 2017. Analysis of the influence of stiffness reduction on the load carrying capacity of ring-stiffened cylindrical shell. *Ocean Eng.* 135, 52–62. doi:10.1016/j.oceaneng.2017.02.034.
- Baruch, M., Singer, J., 1963. Effect of eccentricity of stiffeners on the general instability of stiffened cylindrical shells under hydrostatic pressure. *J. Mech. Eng. Sci.* 5 (1), 23–27. doi:10.1243/JMES.JOUR.1963.005.005.02.
- Belikov, G.I., S.Yu., Kalashnikov, 2011. Layout operation of stiffened cylindrical shells of the bridge conduits under free oscillations. *Bull. Volgograd State Univ. Arch. Civ. Eng., Series. 25* (44), 14–20.
- Block, D.L., Card, M.F., M.M.Jr, Mikulas, August 1965. Buckling of eccentrically stiffened orthotropic cylinders. *NASA TN D-2960*.

- Buragohain, M., Velmurugan, R., 2009. Buckling analysis of Composite hexagonal lattice cylindrical shell using smeared stiffener model. *Defence Sci. J.* 59 (3), 230–238. doi:10.14429/dsj.59.1516.
- Bushnell, D., Bushnell, W.D., 1996. Approximate method for the optimum design of ring and stringer stiffened cylindrical panels and shells with local, inter-ring, and general buckling modal imperfections. *Comput. Struct.* 59 (3), 489–527. doi:10.1016/0045-7949(95)00264-2.
- Chen, B., Liu, G., Kang, J., Li, Y., 2008. Design optimization of stiffened storage tank for spacecraft. *Struct. Multidisc. Optim.* 36, 83–92. doi:10.1007/s00158-007-0174-7.
- Cho, S.-R., Muttaqie, T., Do, Q.T., Park, S.H., Kim, S.M., So, H.Y., Sohn, J.M., 2019. Experimental study on ultimate strength of steel-welded ring-stiffened conical shell under external hydrostatic pressure. *Marine Struct.* 67, 102634. doi:10.1016/j.marstruc.2019.102634.
- Dow N.F., Libove C., Hubka R.E. Formulas for elastic constants of plates with integral waffle-like Stiffening, NACA RM LS3E1 3a, August 1953 <http://ntrs.nasa.gov/archive/nasa/casi.ntrs.nasa.gov/19930090985.pdf>
- Dyachenko, Y.P., Elenitskiy, E.J., Petrov, D.V., 2011. Non-stationary problems of the dynamics of stepped section plates and rotation cylindrical shells. *J. Samara State Tech. Univ., Ser. Phys. Math. Sci.* 2 (23), 278–288.
- Endzhevskiy, L.V., 1982. *Nonlinear Deformation of Ribbed Shells*. Izd-vo of Krasnoyarsk. univ., Krasnoyarsk.
- Hao, P., Wang, B., Tian, K., Liu, H., Wang, Y., Niu, F., Zeng, D., 2017. Simultaneous buckling design of stiffened shells with multiple cutouts. *Eng. Optim.* 49 (7), 1116–1132. doi:10.1080/0305215X.2016.1235328.
- Ilyin, V.P., Karpov, V.V., 1986. *Stability of Ribbed Shells With Large Displacements*. Stroyizdat, Leningrad.
- Jarmai, K., Snyman, J.A., Farkas, J., 2006. Minimum cost design of a welded orthogonally stiffened cylindrical shell. *Comput. Struct.* 84, 787–797. doi:10.1016/j.compstruc.2006.01.002.
- Jaunky, N., December 1992. *Elastic Buckling of Stiffened Composite Curved Panel Master's Thesis*. Old Dominion University, Norfolk, Virginia.
- Jaunky, N., Knight, N.F., Ambur, D.R., 1996. Formulation of an improved smeared stiffener theory for buckling analysis of grid-stiffened composite panels. *Compos Part B-Eng.* 27 (5), 519–526. doi:10.1016/1359-8368(96)00032-7.
- Jones, R.M., 1968. Buckling of circular cylindrical shells with multiple orthotropic layers and eccentric stiffeners. *AIAA J* 6 (12), 2301–2305. doi:10.2514/3.4986.
- Karmishin, A.V., Lyaskovets, V.A., Myachenkov, V.I., Frolov, A.N., 1975. *Statics and Dynamics of Thin-Walled Shell Structures*. Mashinostroenie, Moscow.
- Karpov, V.V., 1999. *Geometrically Nonlinear Problems of Plates and shells, and Methods for Their Solution*. Izd-vo ASV; SPbSUACE, Moscow; Saint-Petersburg.
- Karpov, V.V., 2010. *The Strength and Stability of Reinforced Shells of Revolution: in 2 Parts. Part 1: Models and Algorithms of Research of Strength and Stability of Reinforced Shells of Revolution*. Fizmatlit, Moscow.
- Karpov, V.V., 2011. The strength and stability of reinforced shells of rotation: In 2 parts. Part 2: Computer experiment in static mechanical action. Moscow, Fizmatlit, p. 248 p.
- Karpov, V.V., 2018. Models of the shells having ribs, reinforcement plates and cutouts. *Int. J. Solids Struct.* 146, 117–135. doi:10.1016/j.ijsolstr.2018.03.024.
- Karpov V.V., Petrov V.V. Clarification solutions using stepper methods in the theory of flexible plates and shells. *Izv. ANSSSR, ser. MTT*, 1975, No. 5, P. 189–191.
- Karpov, V.V., Semenov, A.A., 2017. Mathematical models and algorithms for studying strength and stability of shell structures. *J. Appl. Ind. Math.* 11 (1), 70–81. doi:10.1134/S1990478917010082.
- Karpov, V.V., Semenov, A.A., 2018. Dimensionless models of deformation of stiffened shell structures. *PNRPU Mech. Bull.* (1–2) 37–49. doi:10.15593/pern.mech/eng.2018.1.05.
- Kidane, S., Li, G., Helmes, J., Pang, S., Woldesenbet, E., 2003. Buckling load analysis of grid stiffened composite cylinders. *Compos. Part B Eng.* 34, 1–9. doi:10.1016/S1359-8368(02)00074-4.
- Klimanov, V.I., Timashev, S.A., 1985. *Nonlinear Problems of Reinforced Shells*. USC of USSR Academy of Sciences, Sverdlovsk.
- Kuznetsov, E.B., 2012. Continuation of solutions in multiparameter approximation of curves and surfaces. *Comput. Math. Math. Phys.* 52 (8), 1149–1162. doi:10.1134/S0965542512080076.
- Latifov, F.S., Suleymanova, S.G., 2009. A problem of free vibrations medium-filled cylindrical shells reinforced by a cross system of ribs and loaded with axial contracting forces. *Mechanics of machines. Mech. Mater.* 1 (C), 59–61.
- Lee, Y.S., Kim, Y.W., 1998. Vibration analysis of rotating composite cylindrical shells with orthogonal stiffeners. *Comput. Struct.* 69, 271–281. doi:10.1016/S0045-7949(97)00047-3.
- Lee, Y.S., Kim, Y.W., 1999. Effect of boundary conditions on natural frequencies for rotating composite cylindrical shells with orthogonal stiffeners. *Adv. Eng. Softw.* 30, 649–655. doi:10.1016/S0965-9978(98)00115-X.
- Lene, F., Duvaut, G., Olivier-Mailhe, M., Ben Chaabane, S., Grihon, S., 2009. An advanced methodology for optimum design of a composite stiffened cylinder. *Compos. Struct.* 91, 392–397. doi:10.1016/j.compstruct.2009.04.005.
- Lurie, A.I., 1948. *The general equations of the shell, reinforced by stiffening ribs*. Leningrad.
- Lutskaia, I.V., Maksimuk, V.A., Storozhuk, E.A., Chernyshenko, I.S., 2016. Nonlinear elastic deformation of thin composite shells of discretely variable thickness. *Int. Appl. Mech.* 52 (6), 616–623. doi:10.1007/s10778-016-0782-2.
- McElman, J.A., M.M Jr., Mikulas, Stein, M., 1966. Static and dynamic effects of eccentric stiffening of plates and cylindrical shells. *AIAA J.* 4 (5), 887–894. doi:10.2514/3.3562.
- Mehtiyev, M.A., 2011. Nonlinear parametric vibrations of stiffened cylindrical shell with a viscoelastic filler. *Mechanics of machines. Mech. Mater.* 3, 28–30.
- Meish, V.F., Kairov, A.S., 2005. Vibrations of reinforced cylindrical shells with initial deflections under nonstationary loads. *Int. Appl. Mech.* 41 (1), 42–48. doi:10.1007/s10778-005-0056-x.
- Nazarov, N.A., 1965. On vibrations of shallow shells supported by stiffeners. *Appl. Mech.* 1 (3), 24–31.
- Nemchinov Yu., I., Talbatov Yu, A., 1975. Free vibrations of shallow cylindrical shells supported by stiffeners. *Struct. Mech. Struct. Anal.* 3, 17–22.
- Petrov, V.V., 1975. The method of successive loadings in the nonlinear theory of plates and shells. Saratov, Izd. SGU.
- Prusty, B.G., 2008. Free vibration and buckling response of hat-stiffened composite panels under general loading. *Int. J. Mech. Sci.* 50, 1326–1333. doi:10.1016/j.jimecsci.2008.03.003.
- Reddy, A.D., Valisetty Rao, R., Rehfield, L.W., 1985. Continuous filament wound composites concepts for aircraft fuselage structures. *AIAA J. Aircraft* 22, 249–255. doi:10.2514/3.45115.
- Ren, M.F., Li, T., Huang, Q.Z., Wang, B., 2014. Numerical investigation into the buckling behavior of advanced grid stiffened composite cylindrical shell. *J. Reinf. Plast. Compos.* 33 (16), 1508–1519. doi:10.1177/0731684414537881.
- Sadeghifar, M., Bagheri, M., Jafari, A.A., 2011. Buckling analysis of stringer-stiffened laminated cylindrical shells with nonuniform eccentricity. *Arch. Appl. Mech.* 81 (7), 875–886. doi:10.1007/s00419-010-0457-0.
- Semenov, A.A., 2016. Strength and stability of geometrically nonlinear orthotropic shell structures. *Thin-Walled Struct.* 106, 428–436. doi:10.1016/j.tws.2016.05.018.
- Seyfullayev, A.I., Novruzova, K., 2015. Oscillations of a longitudinally reinforced orthotropic cylindrical shell filled with a viscous fluid. *Eastern-Eur. J. Enterprise Technol.* 3/7, 29–33. doi:10.15587/1729-4061.2015.44393.
- Shulga, N.A., S.Yu, Bogdanov, 2003. Forced axisymmetric nonlinear vibrations of reinforced composite shells. *Int. Appl. Mech.* 39 (12), 1447–1451. doi:10.1023/B:INAM.0000020829.56530.22.
- Simoes, L.M.C., Farkas, J., Jarmai, K., 2006. Reliability-based optimum design of a welded stringer-stiffened steel cylindrical shell subject to axial compression and bending. *Struct. Multidisciplin. Optim.* 31, 147–155. doi:10.1007/s00158-005-0592-3.
- Singer, J., Baruch, M., Harari, O., 1967. On the stability of eccentrically stiffened cylindrical shells under axial compression. *Int. J. Solids Struct.* 3, 445–470. doi:10.1016/0020-7683(67)90001-7.
- Smerdov, A.A., 2014. Possibilities of improving the local stability of stiffened and integral composite structures. In: *Proceedings of Higher Educational Institutions. Machine Building.*, 10, pp. 70–79.
- Solovei, N.A., Krivenko, O.P., Malygina, O.A., 2015. Finite element models for the analysis of nonlinear deformation of shells stepwise-variable thickness with holes, channels and cavities. *Mag. Civ. Eng.* 01 (53), 56–69. doi:10.5862/MCE.53.6.
- Suleymanova, S.G., 2007. Free vibrations of a filled cylindrical shell longitudinally strengthened and loaded with axial contracting forces. *Proc. IMM of Azerbaijan XXVII*, 135–140.
- Talebitooti, M., Ghayour, M., Ziaei-Rad, S., Talebitooti, R., 2010. Free vibrations of rotating composite conical shells with stringer and ring stiffeners. *Arch. Appl. Mech.* 80, 201–215. doi:10.1007/s00419-009-0311-4.
- Troitsky, M.S., 1976. *Stiffened Plates, Bending, Stability and Vibrations*. Elsevier Scientific Publishing Company.
- Van der Neut A. The General Instability of Stiffened Cylindrical Shells under Axial Compression, Report S. 314, National Aeronautical Research Institute (Amsterdam) (1947).
- Vlasov, V.Z., 1949. Contact problems in the theory of thin shells and rods. *Proc. of the Acad. of Sci. of the USSR. Dep. of Tech. Sci* 6, 819–939.
- Wang, B., Tian, K., Hao, P., Zheng, Y., Ma, Y., Wang, J., 2016. Numerical-based smeared stiffener method for global buckling analysis of grid-stiffened composite cylindrical shells. *Compos. Struct.* 152, 807–815. doi:10.1016/j.compstruct.2016.05.096.
- Wang, J.T.S., Hsu, T.M., 1985. Discrete analysis of stiffened composite cylindrical shells. *AIAA J* 23, 1753–1761. doi:10.2514/3.9162.
- Xu, Y., Tong, Y., Liu, M., Suman, B., 2016. A new effective smeared stiffener method for global buckling analysis of grid stiffened composite panels. *Compos. Struct.* 158, 83–91. doi:10.1016/j.compstruct.2016.09.015.
- Zhao, X., Liew, K.M., Ng, T.Y., 2002. Vibrations of rotating cross-ply laminated circular cylindrical shells with stringer and ring stiffeners. *Int. J. Solids Struct.* 39, 529–545. doi:10.1016/S0020-7683(01)00194-9.